

FRONTIERS IN PALAEOLOGY

Computational fluid dynamics as a tool for testing functional and ecological hypotheses in fossil taxa

by IMRAN A. RAHMAN

Oxford University Museum of Natural History, Parks Road, Oxford, OX1 3PW, UK; e-mail: imran.rahman@oum.ox.ac.uk

Abstract: Computational fluid dynamics is a method for simulating fluid flows that has been widely used in engineering for decades, and which also has applications for studying function and ecology in fossil taxa. However, despite the possible benefits of this approach, computational fluid dynamics has been used only rarely in palaeontology to date. In this article, I outline the theoretical basis underlying the technique and detail the main steps involved in carrying out computer simulations of fluid flows. I also describe previous studies that have applied the method to fossils and discuss their potential for informing future research directions in palaeontology. Computational fluid dynamics can enable large-scale comparative analyses, as well as exacting tests of hypotheses related to the function and ecology of ancient organisms. In this way, it could transform our understanding of many extinct fossil groups.

Key words: computational fluid dynamics, fossils, function, ecology, hypothesis testing.

25

26 Reconstructing how ancient organisms moved and fed is key to understanding past
27 ecosystems, but is often dismissed as speculative because such inferences can be hard to test.
28 In particular, this work has long been hindered by a lack of objective data on the function of
29 extinct species, especially those without extant analogues. However, the recent development
30 and increasing availability of techniques for visualizing and analysing specimens digitally
31 and in three dimensions, including virtual modelling approaches, provides a quantitative
32 framework for testing specific hypotheses even in problematic fossil taxa. Thus, it is now
33 more feasible than ever before to study the function and ecology of ancient organisms.

34

35 One such method for palaeontological functional analysis is computational fluid dynamics
36 (CFD). CFD is a tool for simulating flows of fluids (liquids or gases) and their interaction
37 with solid surfaces. Complex equations describing the motion of fluids are solved
38 numerically using a computer, and the results can be visualized as plots of fluid properties
39 (e.g. velocity and pressure) within the flow domain. The first computational simulations of
40 fluid flow were undertaken in the 1950s and 1960s (e.g. Evans & Harlow 1957; Harlow &
41 Welch 1965; Hess & Smith 1967), fuelled by the development of increasingly powerful
42 computers. CFD has subsequently been used to analyse design and optimize performance for
43 a wide variety of structures and machines, ranging from nuclear reactors (e.g. Yadigaroglu
44 2005; Mahaffy et al. 2007) to aircraft (e.g. Agarwal 1999; Spalart & McLean 2011), and it is
45 well established in engineering. CFD is also becoming increasingly important in biology and
46 medicine; for example, to study blood flow in the human cardiovascular system (e.g.
47 Migliavacca et al. 2000; Hoi et al. 2004; Young et al. 2014) and the functional performance
48 of flying and swimming animals (e.g. Liu 2002; Kato & Kamimura 2008; Deng et al. 2013).

To date, however, it has been employed only rarely in palaeontology (e.g. Rigby & Tabor 2006; Shiino et al. 2012; Rahman et al. 2015a).

In this paper, I introduce the fundamentals of fluid dynamics and outline the main steps involved in conducting a CFD analysis. I also discuss the applications of CFD to the study of fossil material, encompassing work on extinct vertebrates and invertebrates, as well as different types of flows. This approach has great potential for informing rigorous tests of long-standing functional and ecological hypotheses, and could thus impact on a variety of research directions in palaeobiology.

FLUID DYNAMICS

CFD is an approach in fluid dynamics, which is the branch of fluid mechanics concerned with fluids in motion (as opposed to fluid statics, which deals with fluids at rest). Fluid dynamics relies on three conservation laws of physics: the conservation of mass; the conservation of momentum (Newton's second law); and the conservation of energy. These can be formulated as mathematical equations—such as the Navier–Stokes equations that represent the conservation of momentum and the continuity equation that represents the conservation of mass—which are solved to predict fluid flow. The specific equations used depend on the properties of the fluid; for example, the Navier–Stokes equations are different for compressible (changes in pressure cause changes in density) and incompressible (changes in pressure cause no changes in density) fluids. Liquids are usually treated as incompressible because any density changes are so small as to be negligible; gases are considered as

compressible or incompressible according to the flow velocity (compressible for Mach numbers greater than about 0.3).

The behaviour of the governing equations depends on the contribution of the forces acting on the fluid. These include the inertial forces, which are related to the momentum of the fluid, and the viscous forces, which are frictional forces (shear stress) due to the relative motion of adjacent layers of the fluid. Viscosity is the resistance of the fluid to deformation by these frictional forces. The fluid is said to be Newtonian when the viscosity is constant and non-Newtonian when the viscosity is dependent on the shear rate; air and water are examples of Newtonian fluids, while blood is a non-Newtonian fluid. The velocity of the flow decreases in the immediate vicinity of a solid surface due to increased frictional forces, producing a velocity gradient that reaches zero at the surface. This thin layer of fluid is called the boundary layer.

The dimensionless Reynolds number (Re) is used to characterize the flow and is defined as the ratio between inertial forces and viscous forces:

$$\text{Re} = \frac{\text{inertial forces}}{\text{viscous forces}} = \frac{\rho UL}{\mu}$$

where ρ is the density of the fluid (kg m^{-3}), U is the characteristic velocity (m s^{-1}), L is the characteristic dimension (m) and μ is the dynamic viscosity of the fluid ($\text{kg m}^{-1} \text{s}^{-1}$). When viscous forces are important (i.e. the viscosity is high, the velocity is low and/or the dimension is small), the Reynolds number will be low and the flow laminar, meaning that the fluid flows orderly in parallel layers (Fig. 1A). As inertial forces begin to dominate (e.g. with increasing velocity), the Reynolds number increases and the flow becomes turbulent,

characterized by the formation of eddies and chaotic motion (Fig. 1B) and a steeper velocity gradient in the boundary layer. In laminar flow, there is little mixing between fluid layers, while in turbulent flow, considerable mixing occurs. The exact values, or critical Reynolds numbers, over which the flow regime changes from laminar to turbulent vary on a case-by-case basis, and there is a broad transitional zone in which both types of flow can occur. Laminar flows can be described through the Navier–Stokes equations, but it is computationally infeasible to resolve the spatial and temporal variation of most turbulent flows using these equations. Typically, an alternative approach is required using, for example, the Reynolds-averaged Navier–Stokes (RANS) equations—time-averaged equations for fluid flow—and a mathematical model to predict the effects of turbulence.

Lastly, the effects of time on the flow fluid should be considered. Where the fluid properties are invariant with time, the flow is said to be steady (or stationary). However, if the fluid properties vary with time, the flow is unsteady (or transient). Laminar flows are often steady, whereas turbulent flows are always unsteady. Nevertheless, turbulent flows can be treated as statistically stationary if the mean flow properties do not change with time (Pope 2000). Steady flows are more tractable than unsteady ones, which must incorporate time into calculations and, hence, take significantly longer to solve.

HOW DOES CFD WORK?

There are a variety of commercial (e.g. ANSYS Fluent, Autodesk CFD and COMSOL Multiphysics) and open-source (e.g. Fluidity, OpenFOAM and SU2) software packages for CFD. All these programs share a number of common steps, which are outlined below.

Computational domain

The first step is to create the computational domain, which consists of any objects around/through which the fluid will flow (Fig. 2A). In many cases, these objects are imported from separate computer-aided design (CAD) programs, but simple shapes can be built in the CFD software itself. The dimensionality of the geometry will depend on the objective of the analysis and the available computer power; one- and two-dimensional models are much less computationally expensive than three-dimensional ones, but might not be appropriate for complex shapes that are hard to define with a single line or cross-section, as is often the case for biological and palaeontological specimens. Three-dimensional digital reconstructions are now routinely produced in studies of fossil morphology (Abel et al. 2012; Cunningham et al. 2014; Sutton et al. 2014, 2017), and in many cases these ‘virtual fossils’ will be suitable for use in CFD analyses—albeit after correcting for taphonomic and diagenetic distortion (e.g. Lautenschlager 2016), removing noise and other artefacts and conversion into an appropriate file format for the CFD software. When flow is to be simulated around the exterior of the fossil, internal features are unimportant, and thus reconstructions could be derived from tomographic (e.g. X-ray computed tomography) or surface-based methods (e.g. laser scanning or photogrammetry); however, internal flows (e.g. Bourke et al. 2014) require reconstructions that incorporate interior features, meaning surface-based techniques will be inappropriate. Alternatively, three-dimensional models of fossils can be created through box modelling, which is particularly useful for taxa lacking complete, three-dimensionally preserved specimens (Rahman & Lautenschlager 2017). A plethora of software is available

for digitally reconstructing or modelling fossils in three dimensions (Abel et al. 2012; Cunningham et al. 2014; Sutton et al. 2014, 2017).

In simulations of external flows, the domain surrounding the fossil must also be defined, and this will typically comprise a cuboid or cylinder (for three-dimensional models) (Fig. 2A). The size of the domain should be sufficiently large to allow the flow to fully develop on all sides of the fossil. For example, previous studies (e.g. Shiino et al. 2009, 2012, 2014) used a computational domain that extended three times the length of the fossil upstream, ten times the length of the fossil downstream and five times the size of the fossil in all other directions; however, in some cases it might be possible to accurately resolve the flow using a smaller domain. Sensitivity analyses can be conducted to determine the optimal domain size (see below).

Material properties and flow model

After creating the computational domain, the physical properties (e.g. density and viscosity) of the fluid can be assigned to the model using a built-in materials library or based on values taken from the literature (e.g. Poling et al. 2000). An appropriate flow model is then selected depending on whether the flow regime is characterized as laminar (low Re) or turbulent (high Re). The available flow models (i.e. laminar and different turbulence models, such as the Spalart–Allmaras, k-epsilon and SST models) will differ according to the software used; models vary in terms of the calculations performed to simulate the flow, and choosing between them is partly a compromise between accuracy and computational time/memory. See Wilcox (2006) for an in-depth discussion of alternative turbulence models.

Boundary conditions

Boundary conditions representing flow variables at the boundaries of the domain must be added to the model (Fig. 2A). Typically, an inlet boundary condition is defined at one end of the computational domain, representing net flow into the domain, with an outlet boundary condition at the opposing end of the domain (net outflow). A common configuration for incompressible flows has the velocity specified at the inlet and the pressure fixed at zero at the outlet. The inlet velocity will depend on the palaeobiology and inferred environment of the fossil taxon; in simulations of organisms moving through the flow, comparisons with theoretical or experimentally-derived flying or swimming speeds of extant animals (e.g. Azuma 2006) could provide a realistic range, whereas for stationary organisms, data on water or wind currents in modern environments (e.g. Siedler et al. 2013; Randall 2015) should be consulted. A wall boundary condition describing the fluid velocity at the fluid–solid interface is assigned to all solid surfaces; in most cases (laminar and many turbulence models), a no-slip boundary condition is used, which constrains the fluid velocity at zero relative to the object. For external flows, a slip boundary condition can be assigned to the edges of the domain surrounding the fossil, allowing the flow to pass along the walls without friction.

Discretization

In most cases, the next step is to divide the computational domain into a finite number of discrete cells (i.e. a mesh; Fig. 2B–C). Mesh generation can be automated in many CFD

programs, but manual refinement might be necessary for complicated structures. For three-dimensional models, meshes are made up of simple shapes like tetrahedra or hexahedra, which vary in number and size (including within the same mesh) according to the complexity of the geometry and the flow model; thin layers of prismatic elements can be inserted along the interface between the fluid and the solid (Fig. 2C) to better capture flow in the boundary layer. The governing equations of fluid flow are then discretized so they can be solved on each of the mesh cells. There are a number of different techniques for discretization, the most common of which are the finite-difference, finite-element and finite-volume methods. The CFD software selected governs the discretization method; for example, ANSYS Fluent and OpenFOAM use the finite-volume method, while Autodesk CFD and COMSOL Multiphysics use the finite-element method. Meshless approaches also exist (e.g. smoothed particle hydrodynamics; Monaghan 2005), but are not as widely used at present.

Solver

After completing the steps outlined above, the discretized equations can be solved, and hence fluid flow simulated, using the chosen CFD software. The time required for this will depend on a number of factors, including the complexity of the geometry, the flow model and the mesh, as well as the available computer power. The solver type is also important. When the mean properties of the flow do not change over time (i.e. steady flow), a stationary solver can be used to compute the steady-state solution. In contrast, when the flow properties vary with time (i.e. unsteady flow), a time-dependent solver should be used, which computes the solution at select time steps and therefore requires considerably longer than a stationary solver.

Visualization and post-processing

The results of CFD simulations can be visualized in a variety of different ways. Commonly, plots of flow velocity, pressure or vorticity are created; for time-dependent simulations, these can be generated for different time steps and combined to produce animations. Plots can be supplemented with, for example, streamlines tracing the movement of particles (Fig. 2D). It is also possible to evaluate the forces exerted by the fluid on the fossil, such as the drag (parallel to flow direction) and lift (perpendicular to flow direction) forces. Dimensionless coefficients of drag (C_D) and lift (C_L) can be calculated to facilitate comparisons between models. For three-dimensional models, these are defined as:

$$C_D = \frac{2F_D}{\rho U^2 A}$$

$$C_L = \frac{2F_L}{\rho U^2 A}$$

where F_D is the drag force exerted by the fluid (N), F_L is the lift force exerted by the fluid (N), ρ is the density of the fluid (kg m^{-3}), U is the characteristic velocity (m s^{-1}) and A is the characteristic area (m^2). Depending on the geometry and the flow conditions, the characteristic area is normally the projected frontal area or the surface area.

EXPERIMENTAL COMPARISON AND SENSITIVITY ANALYSIS

CFD is typically cheaper, faster and more flexible than laboratory experiments in flumes or wind tunnels, making it an attractive approach for studying fluid flows. However, comparisons with experimental data are necessary to establish how accurately the computer simulations replicate real-world flow patterns. Studies of this sort are widespread in engineering, especially in the aerospace and automotive industries. They often entail comparing the results of experiments and CFD for benchmark models (e.g. air flow over the Ahmed body, see Ahmed et al. 1984; Lienhart & Becker 2003), but models of more complex geometries can also be utilized (e.g. 3-D printed fossils; Rahman et al. 2015a). The results can be compared qualitatively, or a metric such as the drag coefficient can be used to quantify the extent to which the two methods agree.

Testing the sensitivity of results to changes in the simulation parameters is another important part of a CFD study. The mesh size, in particular, can have a substantial impact on the accuracy of the solution; meshes composed of numerous smaller hexahedral cells with multiple thin prismatic layers at the fluid–solid interface tend to more accurately represent the flow, but require longer simulation times and more computational memory than coarser meshes. Consequently, a sensitivity analysis should be carried out in which simulations are repeated using successively finer meshes in order to establish the coarsest possible mesh size that guarantees the computational accuracy of the CFD simulation, while also minimizing the simulation duration. In certain cases, it will also be necessary to carry out sensitivity analyses to test the influence of other parameters, such as the domain size, flow model or solver type, on the CFD results.

EXAMPLES IN PALAEOLOGY

CFD has much potential for testing hypotheses pertaining to an organism's functional performance, but compared to computer modelling methods like finite-element analysis (e.g. Rayfield 2007; Bright 2014), it has been used infrequently in palaeontology thus far. Rigby & Tabor (2006) were among the first to apply CFD to fossils, simulating laminar flow around two- and three-dimensional models of graptolites (Fig. 3A). Subsequent studies have encompassed computer simulations of laminar and turbulent flows for various fossil invertebrates, including brachiopods (Shiino et al. 2009; Shiino & Kuwazuru 2010, 2011; Shiino & Tokuda 2016), trilobites (Shiino et al. 2012, 2014) and echinoderms (Rahman et al. 2015a; Dynowski et al. 2016; Waters et al. in press), as well as foraminifera (Caromel et al. 2014) and Ediacaran organisms (Rahman et al. 2015b). Vertebrate fossils have also been analysed with CFD: Bourke et al. (2014) simulated internal nasal airflows in the skulls of pachycephalosaurid dinosaurs; Kogan et al. (2015) compared the hydrodynamic performance of the fossil fish *Saurichthys* to a range of extant taxa; and Liu et al. (2015) carried out simulations of water flow around an articulated, free-swimming plesiosaur model.

Initial studies focused on single models, sometimes with a range of inlet velocities. More recently, comparative analyses have become increasingly prominent, exploring the functional performance of alternative life habits (e.g. Shiino et al. 2014; Rahman et al. 2015a; Liu et al. 2015; Dynowski et al. 2016), multiple taxa (e.g. Bourke et al. 2014; Kogan et al. 2015) and real versus hypothetical morphologies (e.g. Shiino & Kuwazuru 2010; Shiino et al. 2012; Rahman et al. 2015b). Such comparative studies can form the basis of rigorous tests of a range of hypotheses relating to the function of fossil taxa. For instance, Shiino et al. (2012) tested the hypothesis that the long, forked hypostome of trilobites aided swimming

performance. In this study, they ran simulations of flow around three-dimensional models of the trilobite *Hypodicranotus striatulus* with and without a hypostome (Fig. 3B). The results showed that the model with a hypostome generated generally lower drag coefficients and more stable lift coefficients than the model without a hypostome, and this suggests that the hypostome played an important role in active swimming. Rahman et al. (2015a) used CFD to test between competing hypotheses for the feeding mode of cinctan echinoderms. They ran simulations for a three-dimensional model of the cinctan *Protocinctus mansillaensis* using different boundary conditions at the mouth to represent either passive or active suspension feeding (Fig. 3C). These simulations showed that there was almost no flow to the mouth in simulations of passive feeding, whereas considerable flow towards the animal was observed for active feeding, supporting the idea that cinctans were active suspension feeders. Liu et al. (2015) tested between alternative theories for the locomotory mode of plesiosaurs. Using a three-dimensional, articulated model of the plesiosaur *Meyerasaurus victor*, they conducted simulations of swimming assuming different ranges of motion for the forelimbs and hindlimbs (Fig. 3D). The results suggested that efficient forward motion entailed using the forelimbs to provide the majority of thrust, with the hindlimbs providing only weak thrust.

FUTURE PROSPECTS

CFD has long been an established method in engineering and has developed as a valuable tool in medicine and biology over the past two decades, but it is only in the last five to ten years that palaeontologists have begun to make use of the approach. In part, this lack of uptake likely reflects the perceived difficulty in applying CFD to fossils; in this paper, I have sought to address this by outlining the main considerations and key steps involved in

performing such analyses. Another obstacle is the cost of the software and hardware needed for CFD, but this can be offset through collaborations with colleagues already working in the field, as well as by making use of open-source software and high-performance workstations optimized for visualizing tomographic data (which are increasingly common in palaeontology research groups). Finally, some researchers might be concerned that simulations do not accurately capture real flow patterns around living, moving organisms. This could be addressed through comparisons with laboratory experiments (see above) and by carrying out computer simulations of articulated models (e.g. Liu et al. 2015) to evaluate the interaction between solid objects in motion and the surrounding fluid. Consequently, the major barriers to using CFD in palaeontology can now be overcome.

The overwhelming majority of palaeontological CFD studies have simulated flows of water around the exterior of fossil organisms (although see Bourke et al. 2014 for one exception). Thus, there is great potential to use CFD to analyse internal fluid flows (e.g. air or blood), as well as for studying the performance of extinct flying organisms, such as pterosaurs. Another area of considerable promise is in using articulated models to explore how flow patterns can vary during locomotion, as pioneered by Liu et al. (2015) in their study of plesiosaur swimming. Such work will enable much more realistic simulations of swimming and flight in fossil taxa, and might even have applications in robotics or the aerospace and automotive industries (i.e. palaeobiomimetics). Lastly, comparative analyses of different fossil taxa, including hypothetical morphologies (e.g. Shiino & Kuwazuru 2010; Shiino et al. 2012; Rahman et al. 2015b), should prove especially informative for addressing outstanding questions in palaeobiology, and will enable thorough tests of evolutionary scenarios. This work is increasingly feasible now that methods for the three-dimensional visualization of

fossils have become a mainstay of palaeontology (Cunningham et al. 2014; Sutton et al. 2014, 2017).

One outstanding challenge for researchers using CFD is establishing how best to make the raw data underlying their work available. Most CFD software generates simulation results in proprietary file formats, which will not be accessible to all potential users. This represents a barrier to the verification and reproducibility of CFD-based studies, while also limiting the possible reuse of datasets arising from this work (e.g. in large-scale comparative analyses).

Ideally, software developers will devise ways to make full details of the computational domain, fluid properties, flow model, boundary conditions and meshes available in accessible file formats. In the meantime, researchers should ensure this information is reported in the methods sections of all relevant publications (Davies et al. in press).

CFD is an extremely powerful approach that can be used to rigorously evaluate functional and ecological hypotheses in ancient organisms, opening up an exciting new avenue in palaeontological functional analysis. Thus far, studies have focused predominantly on analysing water flows around static models of Palaeozoic marine invertebrates, but there is enormous potential for investigating feeding and movement in a wide range of groups in both aerial and aquatic environments. Further work comparing the results of CFD to laboratory experiments will be important for establishing the accuracy of these computational analyses. In the coming years, I anticipate that CFD will become an important part of the palaeontologist's toolkit for addressing questions related to the function of fossil species, transforming our understanding of how ancient organisms moved and fed.

Acknowledgements. I thank Andrew Smith for inviting me to write this review article for the Frontiers in Palaeontology series. I am grateful to Stephan Lautenschlager, Susana Gutarra Díaz, Sally Thomas and two anonymous reviewers, whose comments greatly improved this article. This work was funded by the Royal Commission for the Exhibition of 1851 and the Oxford University Museum of Natural History.

REFERENCES

- ABEL, R. L., LAURINI, C. R. and RICHTER, M. 2012. A palaeobiologist's guide to 'virtual' micro-CT preparation. *Palaeontologia Electronica*, **15**, 6T.
- AGARWAL, R. 1999. Computational fluid dynamics of whole-body aircraft. *Annual Review of Fluid Mechanics*, **31**, 125–169. doi:10.1146/annurev.fluid.31.1.125
- AHMED, S., RAMM, G. and FALTIN, G. 1984. Some salient features of the time-averaged ground vehicle wake. *SAE Technical Paper*, **840300**. doi:10.4271/840300
- AZUMA, A. 2006. *The Biokinetics of Flying and Swimming*. American Institute of Aeronautics and Astronautics, Reston, 514 pp.
- BOURKE, J. M., PORTER, W. R., RIDGELY, R. C., LYSON, T. R., SCHACHNER, E. R., BELL, P. R. and WITMER, L. M. 2014. Breathing life into dinosaurs: tackling challenges of soft-tissue restoration and nasal airflow in extinct species. *The Anatomical Record*, **297**, 2148–2186. doi:10.1002/ar.23046
- BRIGHT, J. A. 2014. A review of paleontological finite element models and their validity. *Journal of Paleontology*, **88**, 760–769.

393 CAROMEL, A. G. M., SCHMIDT, D. N., PHILLIPS, J. C. and RAYFIELD, E. J. 2014.
394 Hydrodynamic constraints on the evolution and ecology of planktic foraminifera. *Marine*
395 *Micropaleontology*, **106**, 69–78.

396 CUNNINGHAM, J. A., RAHMAN, I. A., LAUTENSCHLAGER, S., RAYFIELD, E. J. and
397 DONOGHUE, P. C. J. 2014. A virtual world of palaeontology. *Trends in Ecology and*
398 *Evolution*, **29**, 347–357. doi:10.1016/j.tree.2014.04.004

399 DAVIES, T. G. RAHMAN, I. A., LAUTENSCHLAGER, S., CUNNINGHAM, J. A.,
400 ASHER, R. J., BARRETT, P. M., BATES, K. T., BENGTSON, S., BENSON, R. B. J.,
401 BOYER, D. M., BRAGA, J., BRIGHT, J. A., CLAESSENS, L. P. A. M., COX, P. G.,
402 DONG, X.-P., EVANS, A. R., FALKINGHAM, P. L., FRIEDMAN, M., GARWOOD, R.
403 J. GOSWAMI, A., HUTCHINSON, J. R., JEFFERY, N. S., JOHANSON, Z., LEBRUN,
404 R., MARTÍNEZ-PÉREZ, C., MARUGÁN-LOBÓN, J., O’HIGGINS, P. M., METSCHER,
405 B., ORLIAC, M., ROWE, T. B., RÜCKLIN, M., SÁNCHEZ-VILLAGRA, M. R.,
406 SHUBIN, N. H., SMITH, S. Y., STARCK, J. M., STRINGER, C., SUMMERS, A. P.,
407 SUTTON, M. D., WALSH, S. A., WEISBECKER, V., WITMER, L. M., WROE, S., YIN,
408 Z., RAYFIELD, E. J. and DONOGHUE, P. C. J. In press. Open data and digital
409 morphology. *Proceedings of the Royal Society B*. DENG, H.-B., XU, Y.-Q., CHEN, D.-D.,
410 DAI, H., WU, J. and TIAN, F.-B. 2013. On numerical modelling of animal swimming and
411 flight. *Computational Mechanics*, **52**, 1221–1242. doi:10.1007/s00466-013-0875-2

412 DYNOWSKI, J. F., NEBELSICK, J. H., KLEIN, A. and ROTH-NEBELSICK, A. 2016.
413 Computational fluid dynamics analysis of the fossil crinoid *Encrinus liliiformis*
414 (Echinodermata: Crinoidea). *PLoS ONE*, **11**, e0156408. doi:10.1371/journal.pone.0156408

415 EVANS, M. W. and HARLOW, F. H. 1957. The particle-in-cell method for hydrodynamic
416 calculations. *Los Alamos Scientific Laboratory Report*, **LA-2139**, 76 pp.

417 HARLOW, F. H. and WELCH, J. E. 1965. Numerical calculation of time-dependent viscous
 418 incompressible flow of fluid with free surface. *The Physics of Fluids*, **8**, 2182–2189.
 419 HESS, J. L. and SMITH, A. M. O. 1967. Calculation of potential flow around arbitrary
 420 bodies. *Progress in Aerospace Sciences*, **8**, 1–138.
 421 HOI, Y., MENG, H., WOODWARD, S. H., BENDOK, B. R., HANEL, R. A., GUTERMAN,
 422 L. R. and HOPKINS, L. N. 2004. Effects of arterial geometry on aneurysm growth: three-
 423 dimensional computational fluid dynamics study. *Journal of Neurosurgery*, **101**, 676–681.
 424 doi:10.3171/jns.2004.101.4.0676
 425 KATO, N. and KAMIMURA, S. (eds). 2008. *Bio-mechanics of Swimming and Flying*.
 426 Springer, Tokyo, 403 pp.
 427 KOGAN, I., PACHOLAK, S., LICHT, N., SCHNEIDER, J. W., BRÜCKER, C. and
 428 BRANDT, S. 2015. The invisible fish: hydrodynamic constraints for predator-prey
 429 interaction in fossil fish *Saurichthys* compared to recent actinopterygians. *Biology Open*,
 430 **4**, 1715–1726. doi:10.1242/bio.014720
 431 LAUTENSCHLAGER, S. 2016. Reconstructing the past: methods and techniques for the
 432 digital restoration of fossils. *Royal Society Open Science*, **3**, 160342.
 433 doi:10.1098/rsos.160342
 434 LIENHART, H. and BECKER, S. 2003. Flow and turbulence structure in the wake of a
 435 simplified car model. *SAE Technical Paper*, **2003-01-0656**. doi:10.4271/2003-01-0656
 436 LIU, H. 2002. Computational biological fluid dynamics: digitizing and visualizing animal
 437 swimming and flying. *Integrative and Comparative Biology*, **42**, 1050–1059.
 438 doi:10.1093/icb/42.5.1050
 439 LIU, S., SMITH, A. S., GU, Y., TAN, J., LIU, K. and TURK, G. 2015. Computer
 440 simulations imply forelimb-dominated underwater flight in plesiosaurs. *PLoS*
 441 *Computational Biology*, **11**, e1004605. doi:10.1371/journal.pcbi.1004605

442 MAHAFFY, J., CHUNG, B., DUBOIS, F., DUCROS, F., GRAFFARD, E., HEITSCH, M.,
 443 HENRIKSSON, M., KOMEN, E., MORETTI, F., MORII, T., MÜHLBAUER, P.,
 444 ROHDE, U., SCHEUERER, M., SMITH, B. L., SONG, C., WATANABE, T. and ZIGH,
 445 G. 2007. Best practice guidelines for the use of CFD in nuclear reactor safety applications.
 446 *Nuclear Energy Agency Report, NEA/CSNI/R(2007)5*, 166 pp.

447 MIGLIAVACCA, F., DUBINI, G. and DE LEVAL, M.R. 2000. Computational fluid
 448 dynamics in paediatric cardiac surgery. *Images in Paediatric Cardiology*, **2**, 11–25.

449 MONAGHAN, J. J. 2005. Smoothed particle hydrodynamics. *Reports on Progress in*
 450 *Physics*, **68**, 1703–1759.

451 POLING, B. E., PRAUSNITZ, J. M. and O’CONNELL, J. P. 2000. *The Properties of Gases*
 452 *and Liquids*. McGraw-Hill, New York, 768 pp.

453 POPE, S. B. 2000. *Turbulent Flows*. Cambridge University Press, Cambridge, 771 pp.

454 RAHMAN, I. A., ZAMORA, S., FALKINGHAM, P. L. and PHILLIPS, J. C. 2015a.
 455 Cambrian cinctan echinoderms shed light on feeding in the ancestral deuterostome.
 456 *Proceedings of the Royal Society B*, **282**, 20151964. doi:10.1098/rspb.2015.1964

457 RAHMAN, I. A., DARROCH, S. A. F., RACICOT, R. A. and LAFLAMME, M. 2015b.
 458 Suspension feeding in the enigmatic Ediacaran organism *Tribrachidium* demonstrates
 459 complexity of Neoproterozoic ecosystems. *Science Advances*, **1**, e1500800.
 460 doi:10.1126/sciadv.1500800

461 RAHMAN, I. A. and LAUTENSCHLAGER, S. 2017. Applications of three-dimensional box
 462 modeling to paleontological functional analysis. In TAPANILA, L. and RAHMAN, I. A.
 463 (eds). *Virtual Paleontology. The Paleontological Society Papers*, **22**, 119–132.
 464 doi:10.1017/scs.2017.11

465 RANDALL, D. 2015. *An Introduction to the Global Circulation of the Atmosphere*. Princeton
 466 University Press, Princeton, 456 pp.

- RAYFIELD, E. J. 2007. Finite element analysis and understanding the biomechanics and evolution of living and fossil organisms. *Annual Review of Earth and Planetary Sciences*, **35**, 541–576.
- RIGBY, S. and TABOR, G. 2006. The use of computational fluid dynamics in reconstructing the hydrodynamic properties of graptolites. *GFF*, **128**, 189–194.
- SHIINO, Y., KUWAZURU, O. and YOSHIKAWA, N. 2009. Computational fluid dynamics simulations on a Devonian spiriferid *Paraspirifer bownockeri* (Brachiopoda): generating mechanism of passive feeding flows. *Journal of Theoretical Biology*, **259**, 132–141.
- SHIINO, Y. and KUWAZURU, O. 2010. Functional adaptation of spiriferide brachiopod morphology. *Journal of Evolutionary Biology*, **23**, 1547–1557. doi:10.1111/j.1420-9101.2010.02024.x
- SHIINO, Y. and KUWAZURU, O. 2011. Comparative experimental and simulation study on passive feeding flow generation in *Cyrtospirifer*. *Memoirs of the Association of Australasian Palaeontologists*, **41**, 1–8.
- SHIINO, Y. and TOKUDA, Y. 2016. How does flow recruit epibionts onto brachiopod shells? Insights into reciprocal interactions within the symbiotic framework. *Palaeoworld*, **25**, 675–683.
- SHIINO, Y., KUWAZURU, O., SUZUKI, Y. and ONO, S. 2012. Swimming capability of the remopleuridid trilobite *Hypodicranotus striatus*: hydrodynamic functions of the exoskeleton and the long, forked hypostome. *Journal of Theoretical Biology*, **300**, 29–38. doi:10.1016/j.jtbi.2012.01.012
- SHIINO, Y., KUWAZURU, O., SUZUKI, Y., ONO, S. and MASUDA, C. 2014. Pelagic or benthic? Mode of life of the remopleuridid trilobite *Hypodicranotus striatulus*. *Bulletin of Geosciences*, **89**, 207–218. doi:10.3140/bull.geosci.1409

- 491 SIEDLER, G., GRIFFIES, S. M., GOULD, J. and CHURCH, J. A. (eds) 2013. *Ocean*
 492 *Circulation and Climate: A 21st Century Perspective*. Amsterdam, Academic Press, 904
 493 pp.
- 494 SPALART, P. R. and MCLEAN, J. D. 2011. Drag reduction: enticing turbulence, and then an
 495 industry. *Philosophical Transactions of the Royal Society A*, **369**, 1556–1569.
- 496 SUTTON, M. D., RAHMAN, I. A. and GARWOOD, R. J. 2014. *Techniques for virtual*
 497 *palaeontology*. Wiley, Oxford, 208 pp.
- 498 SUTTON, M. D., RAHMAN, I. A. and GARWOOD, R. J. 2017. Virtual paleontology—an
 499 overview. In TAPANILA, L. and RAHMAN, I. A. (eds). *Virtual Paleontology. The*
 500 *Paleontological Society Papers*, 22, 1–20. doi:10.1017/scs.2017.5
- 501 WATERS, J. A., WHITE, L. E., SUMRALL, C. D. and NGUYEN, B. K. In press. A new
 502 model of respiration in blastoid (Echinodermata) hydrospires based on CFD simulations of
 503 virtual 3D models. *Journal of Paleontology*.
- 504 WILCOX, D. C. 2006. *Turbulence Modeling for CFD*. DCW Industries, La Cañada, 515 pp.
- 505 YADIGAROGLU, G. 2005. Computational fluid dynamics for nuclear applications: from
 506 CFD to multi-scale CMFD. *Nuclear Engineering and Design*, **235**, 153–164.
 507 doi:10.1016/j.nucengdes.2004.08.044
- 508 YOUNG, A., GOURLAY, T., MCKEE, S. and DANTON, M. H. D. 2014. Computational
 509 modelling of the hybrid procedure in hypoplastic left heart syndrome: a comparison of
 510 zero-dimensional and three-dimensional approach. *Medical Engineering & Physics*, **36**,
 511 1549–1553. doi:10.1016/j.medengphy.2014.08.015

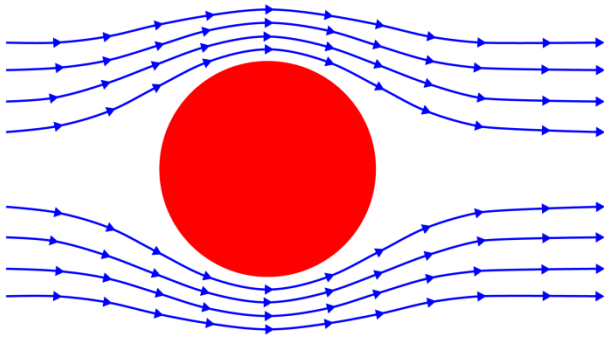
514 **FIGURE CAPTIONS**

Fig. 1. Different types of fluid flows past a cylinder. A, low Reynolds number laminar flow.
B, high Reynolds number turbulent flow.

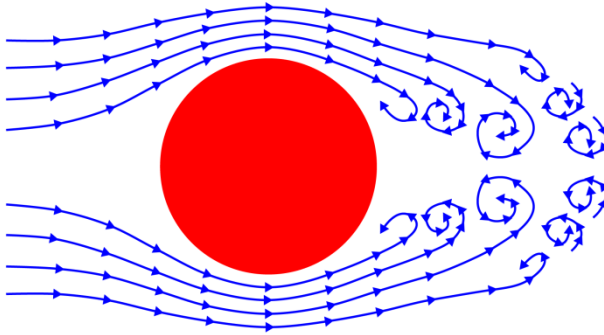
Fig. 2. Main steps in a CFD study using the cinctan *Protocinctus mansillaensis* as an example. A, three-dimensional plot of computational domain with boundary conditions marked. B–C, two-dimensional plots (vertical cross-sections) of mesh used in analysis (red dashed box in B marks the position of C). D, two-dimensional plot (vertical cross-section) of velocity magnitude with streamlines from simulation of water flow.

Fig. 3. Palaeontological CFD analyses. A, three-dimensional plot of velocity contours from simulation of water flow around a model of a fossil graptolite (modified from Rigby & Tabor 2006, fig. 7). B, two-dimensional plots (horizontal and vertical cross-sections) of streamlines from simulations of water flow around models of the trilobite *Hypodicranotus striatulus* with (left) and without (right) a hypostome (modified from Shiino et al. 2012, fig. 5). C, two-dimensional plots (horizontal cross-sections) of velocity magnitude with flow vectors and streamlines from simulations of water flow around models of the cinctan *Protocinctus mansillaensis* assuming passive (top) and active (bottom) suspension feeding (modified from Rahman et al. 2015a, fig. 2). D, three-dimensional plots of tip traces from simulations of water flow around free-swimming models of the plesiosaur *Meyerasaurus victor* assuming narrow (top) and medium (bottom) ranges of motion (modified from Liu et al. 2015, fig. 4).

A



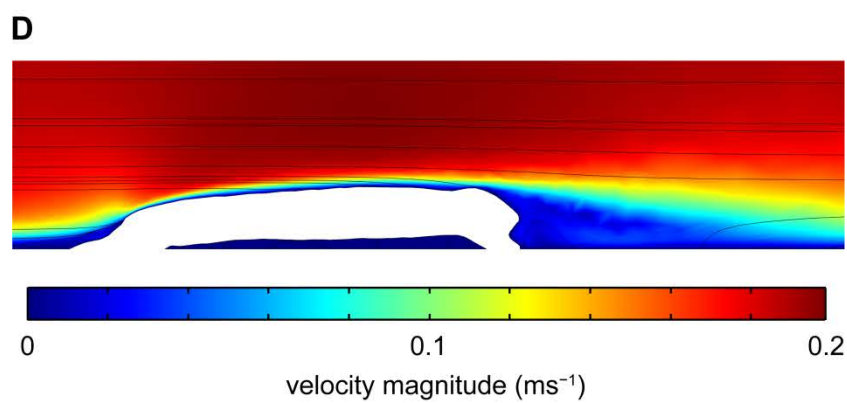
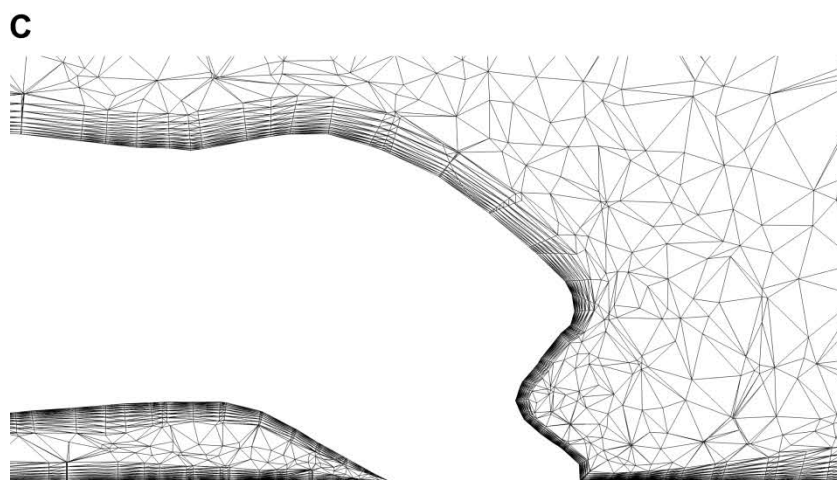
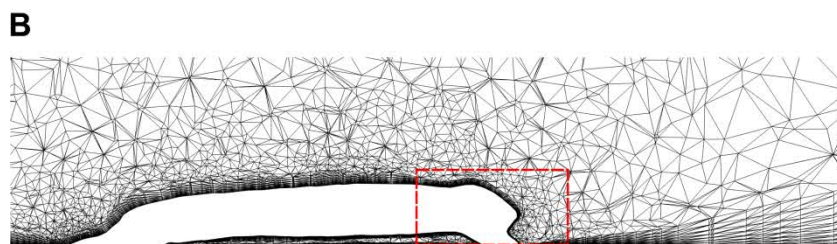
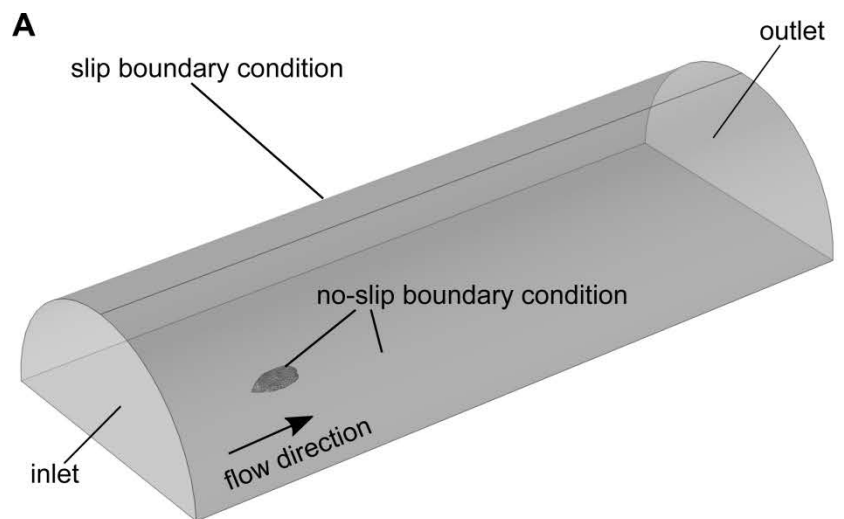
B



537

538 Figure 1.

539



540

541 Figure 2.

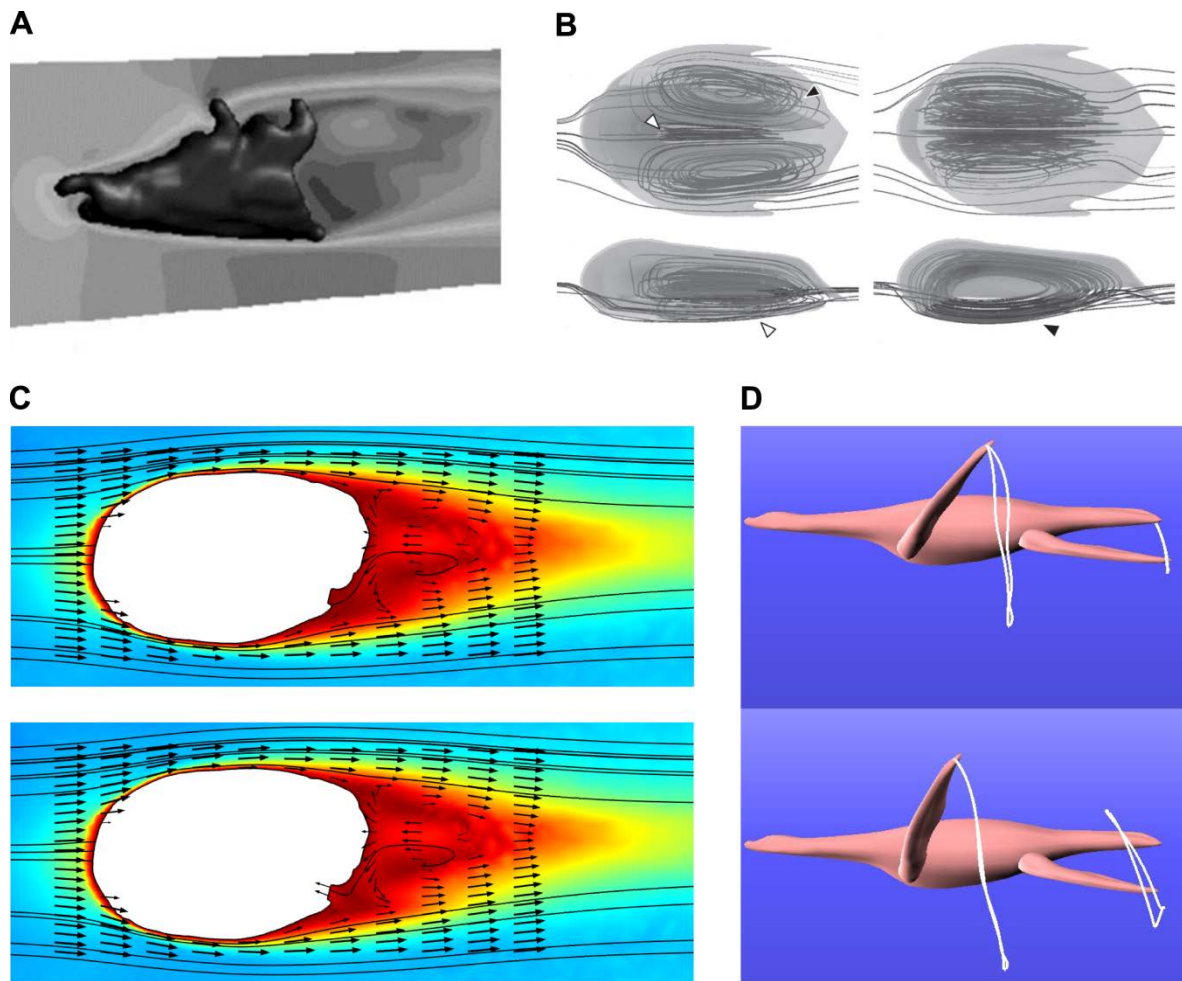


Figure 3.